Available online at www.sciencedirect.com
SCIENCE DIRECT®
Journal of Sound and Vibration 279 (2005) 969–991
JOURNAL OF SOUND AND VIBRATION
www.elsevier.com/locate/jsvi

In-plane dynamic behavior of cable networks. Part 1: formulation and basic solutions

L. Caracoglia, N.P. Jones*

Department of Civil and Environmental Engineering, University of Illinois, Urbana, IL 61801, USA

Received 20 December 2001; accepted 25 November 2003

Abstract

This paper is motivated by mitigation of oscillation of the stays in cable-stayed bridges in which transverse elements (cross-ties) are placed among different stays. The dynamic behavior of a simplified cable network, composed by a set of interconnected truss elements, has been investigated analytically. Solutions to the free-vibration problem have been computed by means of a general analytical procedure. Several special cases have been defined and solved in closed form, revealing interesting characteristics. These examples have been investigated in detail as a background for understanding more complex systems. It is worth noting that even for a relatively modest number of interconnected elements, considerable complexity, which demands a numerical solution technique, is often present. The approach presented herein will be applied to more general configurations and bridge application examples in a companion paper.

1. Introduction

The problem of large-amplitude vibrations on a system of stays on a cable-stayed bridge is a topic that is currently interesting many researchers. One of the methods that is sometimes adopted to counteract the undesired oscillations, usually induced by a combination of wind loads or wind-rain effects [1,2] is to increase the in-plane stiffness of stays by connecting them together by means of a set of transverse cables, defined as cross-ties (or "aiguilles"). According to Ref. [3], these cables are also used to reduce the cable sag variations among the stays of different length, ensuring a more uniform axial stiffness on the consecutive stays. From the dynamic perspective, the properties of the single cable, considered as a separate element, are modified by the presence of

*Corresponding author. Tel.: +1-217-333-9896; fax: +1-217-265-0318.
E-mail address: npjones@uiuc.edu (N.P. Jones).

0022-460X/$ - see front matter © 2003 Elsevier Ltd. All rights reserved.
doi:10.1016/j.jsv.2003.11.058

the lateral constraints that influence its oscillation characteristics. Similarly, a connection of simple suspended elements is transformed into a more complex cable network; a closed-form solution to the dynamic problem is more elusive.

The literature contains examples of performance improvement for a vibrating cable; for example, the widely studied case of adding a transverse damper [4]. However, it is evident that detailed studies of cross-ties and interconnected cable systems are not well reported and most of the recommendations that are currently followed seem to be linked to practice or previous experience. A fundamental study to support these problems seems therefore necessary. It is worth mentioning that a cable network can be a very complex system and finite element analysis has been preferred in the past. An example was given by Ehsan and Scanlan [5], who used component-mode synthesis and finite element approaches for the solution of a three-dimensional cable problem. Reviews of cable vibration that address the most commonly used techniques for reducing motion amplitudes also identify this problem as one that still needs to be investigated [6].

Experience gained in the field of transverse restrainers was analyzed by Virlogeux [7] who points out recent failures or unexpected behavior of the cross-ties (Pont de Normandie, Foro Bridge in Denmark). He addressed the issues of transverse cable stiffness, tension and internal damping. He also suggests that simplified approaches (equivalent static analyses) can be sometimes efficient in terms of design recommendations.

Yamaguchi and Jayawardena [8] and Yamaguchi and Nagahawatta [9] analyzed the problem through a set of experiments conducted on a model of two interconnected cables, and a subsequent finite element simulation of the configuration. An energy approach for the determination of the damping contribution linked to the complex network was used. Among their comments, it is interesting to emphasize that the contribution to damping, due to cross-ties, can be negative or positive, depending on the chosen system and cable characteristics and that not only the overall stiffer configuration must be considered but also the possibility of exploiting the energy dissipation potential of the restrainers.

Several examples of vibration analysis of cable nets were found in the literature, even though most of them are related to high-tension systems, in which the excitation force is mainly orthogonal to the net configuration (i.e., membrane behavior—e.g., Ref. [10]). In most cases a finite element analysis was performed. An interesting approach for the out-of-plane vibration analysis of a non-linear cable system was applied by Mesarovic and Gasparini [11] to the study of a complex truss.

The contribution of the present paper is focused on the development of an analytical method and efficient numerical procedure that models the in-plane behavior of a set of interconnected cables. Observations on the behavior of these cross-tied systems are investigated through the detailed study of specific examples.

2. General problem formulation

Since few relevant examples of in-plane cable network free-vibration analysis were found in the literature in which the problem is also treated in closed form, an analytical study was considered useful for the elaboration and understanding of the more complex system performance. The goal

of this investigation was to better understand the basic mechanics of the phenomenon, when an interaction among independent cable elements is effected by the presence of cross-connections (rigid or non-rigid).

The basic problem analyzed in this work is founded on the behavioral assumption of a highly pre-stressed set of cables, compared to their mass and elastic stiffness, so that the assumption of the taut flat cable can be considered reasonable. The use of this theory [12] also allows for a simplification of dynamic equations: each cable can be considered as extensible, but the stretch exerted to resist the external applied load is of second order in the additional deflection. This implies the absence of dynamic additional tension with respect to the static analysis in the case of the free-oscillation investigation [12]. It is clear that these simplifications can lead to an approximation of a real system; however recent papers, for example by Main and Jones [4], have suggested that a similar approach for the solution of a damped taut cable is reasonable in the context of stay-cable vibration mitigation in bridges.

The initial problem formulation is depicted in Fig. 1. The example shows a simplified network, defined by a set of two taut cables, connected by means of a vertical rigid rod (to be relaxed later). The generic jth cable is divided into m segments, each of which is labeled as p (the generic element is denoted by j,p). The jth cable is restrained at both ends; it is characterized by a length L_j, with $L_1 > L_2$ in this case, tension H_j and mass per unit length μ_j. The horizontal offset between the two cables has been denoted by l_1 and the position of the vertical connection, with respect to the right-hand side of cable "2" has been assumed equal to l_2 (segment 2,1). The quantity $l^* = l_1 + l_2$ represents the same dimension in the coordinate system of the upper cable. The x_{jp} along-axis coordinate of the pth segment of the jth cable has been taken in accordance with Fig. 1. Vertical displacements are considered positive downwards. The position of the vertical connector relative to the cable is general, and the only additional physical constraints are expressed by $L_2 \leqslant L_1$; $l_2 \leqslant L_2$; $l_1 + L_2 \leqslant L_1$. A primary nomenclature is used in this section for the description of general approach; a secondary and simplified notation (in parentheses) is also indicated and will be used in Sections 3 and 4.

The solution to the free-vibration problem is concerned with a system of four partial differential equations, corresponding to the four cable branches $y_{jp}(x_{jp}, t)$, with $j = 1, 2$ and

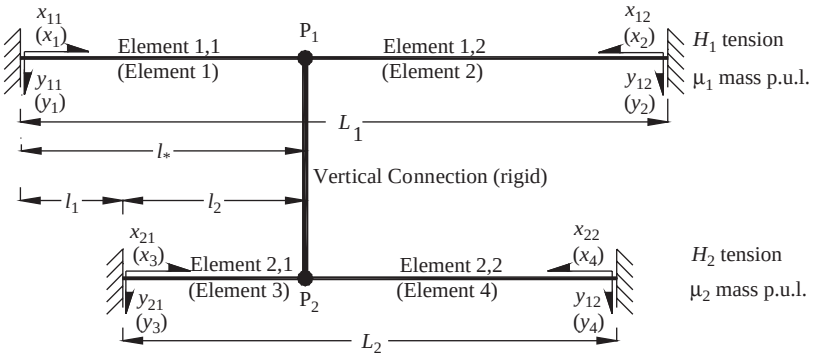

Fig. 1. General problem formulation (secondary notation in parentheses).

$p = 1, 2$, where t denotes the time variable:

$$H_j \frac{\partial^2 y_{jp}}{\partial x_{jp}^2} = \mu_j \frac{\partial^2 y_{jp}}{\partial t^2}, \tag{1}$$

where $j = 1, \ldots, n$ is the number of cables and $p = 1, \ldots, m$ the number of segments, for each cable.

This system requires eight boundary, compatibility and equilibrium conditions, which can be expressed in terms of (1) displacements at cable ends; (2) displacement continuity at point $P1$ between elements "1,1" and "1,2", and at $P2$ for segments "2,1" and "2,2"; (3) equality of displacement at each time instant at $P1$ and $P2$ between the two cables; (4) force equilibrium at the vertical rod. These can be written as

$$y_{jp}(x_{jp} = 0, t) = 0 \quad \text{for } j = 1, 2 \text{ and } p = 1, 2, \tag{2a}$$

$$y_{11}(x_{11} = l^*, t) = y_{12}(x_{12} = L_1 - l^*, t), \quad y_{21}(x_{21} = l_2, t) = y_{22}(x_{22} = L_2 - l_2, t), \tag{2b}$$

$$y_{11}(x_1 = l^*, t) = y_{21}(x_3 = l_2, t), \tag{2c}$$

$$H_1 \left(\left.\frac{\partial y_{11}}{\partial x_{11}}\right|_{x_1 = l^*} + \left.\frac{\partial y_{12}}{\partial x_{12}}\right|_{x_2 = L_1 - l^*} \right) + H_2 \left(\left.\frac{\partial y_{21}}{\partial x_{21}}\right|_{x_3 = l_2} + \left.\frac{\partial y_{22}}{\partial x_{22}}\right|_{x_4 = L_2 - l_2} \right) = 0. \tag{2d}$$

A purely oscillatory motion of each cable element can be developed using the Bernoulli–Fourier method in which time-dependent and spatial-co-ordinate effects can be separated as $y_{jp}(x_{jp}, t) = Y_{jp}(x_{jp}) e^{i\omega t}$, where ω is the natural circular frequency of vibration of the coupled network (unknown). Eqs. (1) can be therefore reduced to a system of ordinary equations:

$$H_j \frac{d^2 Y_{jp}}{dx_{jp}^2} + \mu_j \omega^2 Y_{jp} = 0 \quad (j = 1, 2,\ p = 1, 2). \tag{3}$$

From Eq. (3) and conditions (2a) the solution can be proposed of the form

$$Y_{11,12}(x_{11,12}) = A_{11,12} \sin\left(\frac{\alpha\pi}{L_1} x_{11,12}\right), \quad Y_{21,22}(x_{21,22}) = A_{21,22} \sin\left(\frac{\alpha f \pi}{L_1} x_{21,22}\right). \tag{4a, b}$$

In Eqs. (4) the upper cable is considered as reference element; α represents the reduced frequency of the system, and f is a parameter that takes into account geometrical and stiffness differences of cable "2" with respect to "1", defined as scaled frequency ratio. From Eqs. (3) such quantities can be redefined according to

$$\omega = \alpha \frac{\pi}{L_1} \left(\frac{H_1}{\mu_1}\right)^{1/2} = \alpha\omega_{01}, \quad f = \left(\frac{H_1}{H_2}\right)^{1/2} \left(\frac{\mu_2}{\mu_1}\right)^{1/2} = \frac{\omega_{01}}{\omega_{02}} \frac{L_1}{L_2}. \tag{5}$$

In these equations ω_{01} and ω_{02} are the fundamental circular frequencies of the unconnected cables. Eqs. (4a) and (4b) generally satisfy the requirements of system (3). The unknown parameters A_{jp}, representing the four modal amplitudes of each pth segment, must be solved from the four boundary conditions (2b–2d). In this way the solution to the free-oscillation problem, and the determination of the natural frequencies in terms of α, can be transformed into a system

of four algebraic equations, linked to (2b–2d), in matrix form

$$\mathbf{SA} = \mathbf{0}, \quad \mathbf{A} = [A_{11}\ A_{12}\ A_{21}\ A_{22}]^{\mathrm{T}}, \tag{6a, b}$$

$$\mathbf{S} = \begin{Bmatrix} \sin(\alpha\pi\xi_1) & -\sin[\alpha\pi(1-\xi_1)] & 0 & 0 \\ 0 & 0 & \sin(\alpha\pi\Delta\xi) & -\sin\left[\alpha f\pi\left(\dfrac{L_2}{L_1}-\Delta\xi\right)\right] \\ \sin(\alpha\pi\xi_1) & 0 & -\sin(\alpha f\pi\Delta\xi) & 0 \\ \cos(\alpha\pi\xi_1) & \cos[\alpha\pi(1-\xi_1)] & \dfrac{f}{h}\cos(\alpha f\pi\Delta\xi) & \dfrac{f}{h}\cos\left[\alpha f\pi\left(\dfrac{L_2}{L_1}-\Delta\xi\right)\right] \end{Bmatrix}, \tag{6c}$$

where all quantities have been reduced into the following dimensionless parameters: $h = H_1/H_2$; $\xi_1 = l_*/L_1$; $\xi_2 = l_1/L_1$; $\Delta\xi = l_2/L_1 = (\xi_1 - \xi_2)$. The infinite set of non-trivial solutions ($\mathbf{A} \neq \mathbf{0}$) to the homogeneous system (6a) can be identified through the condition $\det[\mathbf{S}] = 0$. This condition is given by the roots of the following polynomial $p(\alpha)$:

$$p(\alpha) = \sin(\alpha\pi)\left\{\cos\left[\alpha f\pi\left(2\Delta\xi - \frac{L_2}{L_1}\right)\right] - \cos\left(\alpha f\pi\frac{L_2}{L_1}\right)\right\} + \frac{h}{f}\sin\left(\alpha f\pi\frac{L_2}{L_1}\right)\{\cos(2\alpha\pi\xi_1 - \alpha\pi) - \cos(\alpha\pi)\}. \tag{7}$$

Eq. (7) represents the frequency equation that relates the general solution to a specific value of the system reduced frequency α, for which the modal amplitudes of the rth segment can be obtained through the linearly independent equations (6). The roots of Eq. (7) cannot be found analytically in closed form for the general case, since little further simplification is possible; a numerical technique can be adopted in this general case. Prior to the implementation of this general approach, however, the study of some sample cases, in which the trigonometric expressions could be simplified, was performed. A collection of relevant examples was constructed, both to identify the physical behavior and to reveal any interesting characteristics. These are: (1) study of a perfectly symmetric cable system with equal cable elements and locations (twin-cable system) and rigid connection at mid-span; (2) study of a perfectly symmetric cable system with equal cable elements and locations (twin-cable system) and with variable position of the rigid connection; (3) study of a symmetric cable system, in which cable elements have different length but equal mass and tension characteristics and rigid connection at mid-span; (4) same as case (1) but with a non-rigid connection at mid-span (linear spring model); (5) same as case (3) but with a non-rigid connection at mid-span (linear spring model); (6) same as case (5) with an additional extension to ground.

A further extension of the theory will be developed later, in the context of examples 4–6. Examples 1–3 are discussed in Section 3, examples 4–5 in Section 4 and example 6 in Section 5.

3. Rigid connectors

In this section two-cable systems connected by a rigid secondary restrainer were analyzed. Since the number of segments involved is reduced, a modification to the initial convention is introduced

to simplify the notation in Eqs. (4) and (6). Following the secondary nomenclature in Fig. 1, four cable elements are defined (through $r = 1,2,3,4$) and the co-ordinates and parameters that belong to each of them are assumed as $Y_{1\ldots4}$; $x_{1\ldots4}$; $\mathbf{A} = [A_1\ A_2\ A_3\ A_4]^{\mathrm{T}}$.

3.1. Twin-cable system with rigid connection at mid-span

In a perfectly symmetric system the natural frequencies of the isolated cables, 1 and 2, are coincident: $\omega_{01} = \omega_{02}$ ($H_1 = H_2 = H$; $\mu_1 = \mu_2 = \mu$; $L_1 = L_2 = L$). The reduced frequencies of the individual cable, α_{SA}, are equal to the infinite sequence of natural numbers $(1, \ldots, N)$, being the even values corresponding to the symmetric modes and the odd ones to the antisymmetric components [12]. Since $l_2 = l^* = L/2$ and $l_1 = 0$ the dimensionless quantities become $f = h = 1$, $\xi_1 = 1/2$; $\xi_2 = 0$; $\Delta\xi = \xi_1$. The matrix (6c) can be reduced to the form

$$\mathbf{S} = \begin{Bmatrix} \sin\beta & -\sin\beta & 0 & 0 \\ 0 & 0 & \sin\beta & -\sin\beta \\ \sin\beta & 0 & -\sin\beta & 0 \\ \cos\beta & \cos\beta & \cos\beta & \cos\beta \end{Bmatrix} \quad \text{with } \beta = \frac{\alpha\pi}{2}. \tag{8}$$

The characteristic polynomial (7) can be rewritten as

$$p(\alpha) = \{\sin(\alpha\pi)\}\{\cos(\alpha\pi) - 1\}. \tag{9}$$

In solving Eq. (9) two sets of solution can be detected, each of which is related to the vanishing of the quantities in brackets. The first branch, connected to the sine expression, represents the same frequencies as the individual-cable case, α_{SA}; as expected $\alpha_{SA} = k$, with $k = 1, 2, \ldots, N$. The second set is linked to the even-valued solutions of the first series, corresponding to antisymmetric modes of the single cable: in this case a new configuration with the same frequency can be detected.

In particular, from the analysis of Eq. (8) it can be seen that when the reduced frequency is the set of odd numbers, the fourth equation degenerates to the null identity; the modal amplitudes of each rth segment are the same (in-phase motion), corresponding to the symmetric modes of the single cable. No force is exerted by the vertical connection, since the derivatives of Eqs. (4a) and

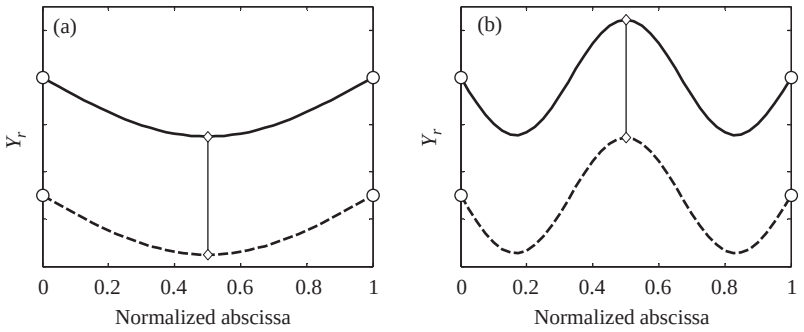

Fig. 2. Y, symmetric eigenfunctions for a twin-cable system with $\xi_1 = 0.50$: (a) 1st symmetric mode, $\alpha = 1$; (b) 3rd symmetric mode, $\alpha = 3$. Solid line: "Cable 1"; dashed line: "Cable 2".

(4b) vanish at mid-span. The general pattern of these modes is represented in Fig. 2 for $k = 1$ (1st symmetric mode, Fig. 2(a), $k = 3$ (3rd symmetric mode, Fig. 2(b)); the vector of normalized modal amplitudes is equal to $\mathbf{A} = 0.5[1\ \ 1\ \ 1\ \ 1]^{\mathrm{T}}$.

When α is even the first three rows in Eq. (8) are identically zero and the solution to the linearly dependent system (6a) can be obtained through the fourth equation with now three unknowns (one of the amplitudes assumed equal to the unit value), corresponding to a root with multiplicity 3. With the modal frequency the same, three independent modal solutions can be found:

- $\mathbf{A}_{AS-I} = 0.5[1\ \ -1\ \ 1\ \ -1]^{\mathrm{T}}$; antisymmetric modes with in-phase motion between upper and lower cables ($\alpha = 2k$, with $k = 1, 2, \ldots, N$)—Fig. 3(a),
- $\mathbf{A}_{AS-II} = 0.5[1\ \ -1\ \ -1\ \ 1]^{\mathrm{T}}$; antisymmetric modes with the two cables (upper and lower) out of phase ($\alpha = 2k$, with $k = 1, 2, \ldots, N$)—Fig. 3(a);
- $\mathbf{A}_{S} = 0.5[1\ \ 1\ \ -1\ \ -1]^{\mathrm{T}}$; symmetric modes (also corresponding to the first set of solutions), in which the two cables are out of phase ($\alpha = 2k$, with $k = 1, 2, \ldots, N$)—Fig. 3(b).

For the two antisymmetric solutions (AS-I and AS-II; Fig. 3(a), the position of P_1 and P_2 nodes is unmodified during the oscillation and no force is transferred through the restrainer.

The modal behavior of $\mathbf{A}_S$ in Fig. 3(b) can also be interpreted as "pseudo-symmetric", due to the discontinuity at nodes P_1 and P_2 (lying on the horizontal axis); in this case, an internal force proportional to $2A_{S,1}\cos(\alpha\pi/2)$, with $A_{S,1}$ modal amplitude of the single cable segment (the same on each element), is present.

The orthogonality among different modes is trivially verified; the three eigenvectors associated with the multiple root form a basis of the space of the solutions, i.e., their linear combination also represents a possible modal form. For example $[1\ \ -1\ 0\ 0]^{\mathrm{T}}$, given by $(\mathbf{A}_{AS-I} + \mathbf{A}_{AS-II})$, corresponds to an eigenfunction in which the lower cable is at rest and $[1\ 0\ 0\ \ -1]^{\mathrm{T}} = (\mathbf{A}_{AS-I} + \mathbf{A}_{S})$ to a mode in which two opposite cross-segments are only responding out of phase.

3.2. Twin-cable system with arbitrary location of the rigid connection

The twin-cable configuration, analyzed in Section 3.1, was extended to the case of an arbitrary location of the rigid restrainer, i.e., by considering $\Delta\xi = \xi_1$, with $0 \leqslant \xi_1 \leqslant 1$. Matrix (6c) can be

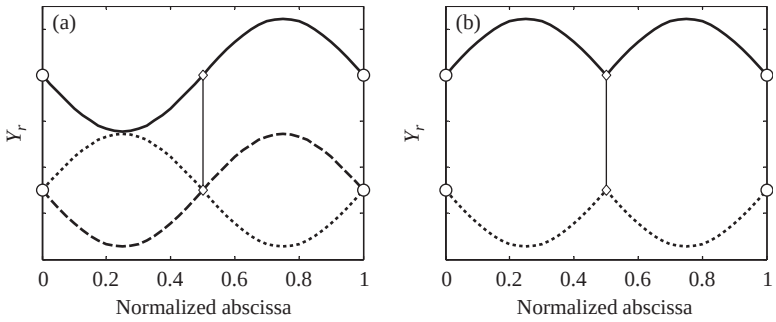

Fig. 3. Twin-cable system with $\xi_1 = 0.50$ and multiple eigenfunctions, Y_r, for $\alpha = 2$: (a) 1st antisymmetric mode; (b) 2nd symmetric mode. Solid line: "Cable 1"; dashed line: "Cable 2" in phase; dotted line: "Cable 2" out of phase.

reduced to the form

$$\mathbf{S} = \begin{Bmatrix} \sin(\alpha\pi\xi_1) & -\sin[\alpha\pi(1-\xi_1)] & 0 & 0 \\ 0 & 0 & \sin(\alpha\pi\xi_1) & -\sin[\alpha\pi(1-\xi_1)] \\ \sin(\alpha\pi\xi_1) & 0 & -\sin(\alpha\pi\xi_1) & 0 \\ \cos(\alpha\pi\xi_1) & \cos[\alpha\pi(1-\xi_1)] & \cos(\alpha\pi\xi_1) & \cos[\alpha\pi(1-\xi_1)] \end{Bmatrix}, \tag{10}$$

and the characteristic polynomial (7) can be written as

$$p(\alpha) = \{\sin(\alpha\pi)\}\{2[\cos(2\alpha\pi\xi_1 - \alpha\pi) - \cos(\alpha\pi)]\}. \tag{11}$$

Two sets of solutions can be detected from Eq. (11), each one of which is related to the vanishing of the quantities in brackets.

The first set (labeled as "S-A"), is connected to the condition $\sin(\alpha\pi) = 0$, similarly to Section 3.1, with reduced frequency $\alpha = k$ ($k = 1, 2, \ldots, N$), equivalent to the isolated-cable case. The odd values of the roots of "S-A" ($\alpha = k$, with $k = 1, 3, 5, \ldots$) correspond to a set of symmetric modes. In system (10) the fourth equation is reduced to a null identity and therefore, the normalized modal amplitudes (in-phase motion) are $\mathbf{A} = 0.5[1\ 1\ 1\ 1]^{\mathrm{T}}$. The even values of this set ($\alpha = k$, with $k = 2, 4, 6, \ldots$) are coincident with the antisymmetric solution of Section 3.1 with in phase contributions from both cables (no multiplicity due to spatial non-symmetry) and no force transferred through the restrainer. The reduction of rank to one for antisymmetric modes is not possible, unless ξ_1 is assumed such that $\sin(\alpha\pi\xi_1) = 0$, for $\alpha = 2k$ (with $k = 1, 2, \ldots, N$). This configuration occurs for "even-valued" ($\alpha = 2k$) higher modes, when $\alpha\xi_1\pi = j\pi$ ($j = 1, 2, 3, \ldots, N$ and $0 \leqslant \xi_1 \leqslant 1$), i.e., for a given α, when

$$\xi_{1,j}(\alpha) = \frac{j}{\alpha} \quad \text{with } j \in \left\{ 1, \ldots, N; \frac{j}{\alpha} < 1 \right\}. \tag{12}$$

This corresponds, as an example, to the locations $\xi_1 = 1/4, 1/2, 3/4$, for $\alpha = 4$. It is clear that, when the position of the strut is coincident with the nodes of a particular modal configuration of the individual cable, a multiple solution (in-phase and out-of-phase antisymmetric) reappears for that frequency.

The second set ("S-B"), associated with $[\cos(2\alpha\pi\xi_1 - \alpha\pi) - \cos(\alpha\pi)] = 0$, generate two subsets of pseudo-symmetric modes, defined as (primary) pseudo-symmetric (PS) and (complementary) pseudo-symmetric (CPS); frequencies and modal normalized amplitudes are respectively defined by the formulae

$$\alpha_{PS} = \frac{k}{1-\xi_1} \quad \text{with } k = 1, 2, \ldots, N, \qquad \mathbf{A}_{PS} = 0.71[0\ 1\ 0\ -1]^{\mathrm{T}}, \tag{13a, b}$$

$$\alpha_{CPS} = \frac{k}{\xi_1}, \quad \text{with } k = 1, 2, \ldots, N, \qquad A_{CPS} = 0.71[1\ 0\ -1\ 0]^{\mathrm{T}}. \tag{14a, b}$$

In both cases the rank of $\mathbf{S}$ is reduced by one: the modal forms are both characterized by zero amplitude on two opposite segments of the twin-cable system, and two remaining symmetric components (out of phase). For a given k, the wavelengths of Eq. (13) are longer than those of Eq. (14), being α associated with a lower frequency. In Figs. 4(a) and (b) the eigenfunctions associated with Eqs. (13) and (14), respectively, are depicted for $k = 1$ and $\xi_1 = 0.35$. A similar

property, as in Eq. (12), can be shown for higher modes and Eqs. (13) for CPS modes, for selected values of ξ_1, i.e., when a triple-multiplicity solution is recovered.

Fig. 5 summarizes the reduced frequency evolution of all different modal forms, as a function of ξ_1 (symmetric, "S"; antisymmetric, "AS"; pseudo-symmetric, "PS" and "CPS"), for the fundamental modes of the twin-cable system. The symmetry of functions (13a) and (14a) with respect to the centerline is evident. Two types of intersections can be seen; those points denoted by "**a**" represent the convergence of three modal frequencies to a unique value (pseudo-symmetric—primary and complementary; antisymmetric), i.e., a triple-multiplicity solution for $\xi_1 = 1/2$, as presented in Section 3.1.

The second class of points ("**b**") are given by the coexistence between a lower order complementary pseudo-symmetric mode, a higher order pseudo-symmetric, and a symmetric mode (Fig. 6(a)). In this case, it is possible to define

$$\upsilon = \frac{k_{CPS}}{k_{PS}} = \frac{\xi_1}{1-\xi_1} < 1, \tag{15}$$

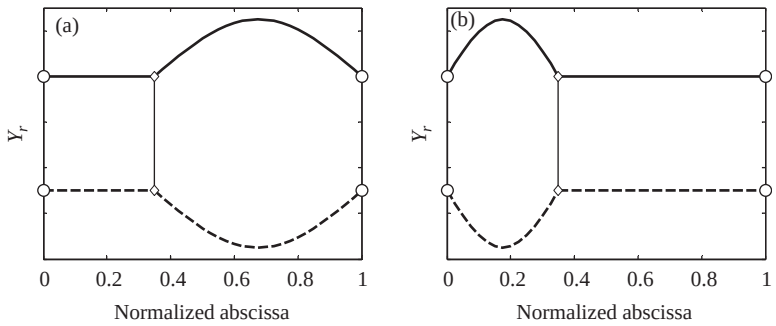

Fig. 4. "S-B" eigenfunctions for a twin-cable system with $\xi_1 = 0.35$; (a) 1st pseudosymmetric mode, $\alpha = 1/(1-\xi_1)$; (b) 1st complementary pseudo-symmetric mode, $\alpha = 1/\xi_1$. Solid line: "Cable 1"; dashed line: "Cable 2".

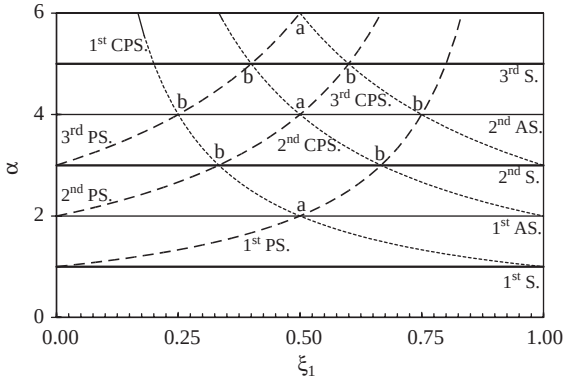

Fig. 5. Reduced frequencies α as a function of the connection location ξ_1 for a twincable system: symmetric ("S", solid thick line), antisymmetric ("AS", solid thin line), pseudo-symmetric ("PS", dashed thick line) and "complementary" pseudo-symmetric ("CPS", dashed thin line) modes.

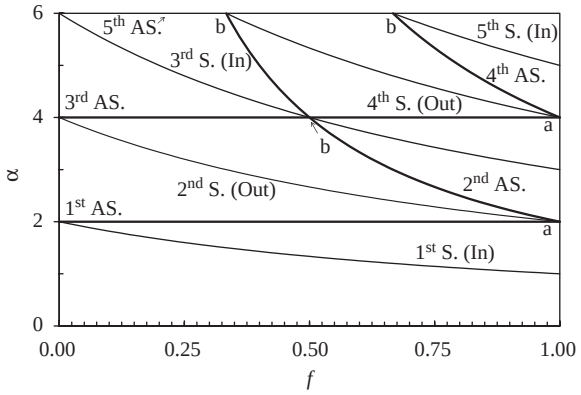

Fig. 6. Rigid-connector symmetric-cable system; reduced frequencies α as a function of the cable length ratio f: symmetric (“S”, solid thin line; “In” phase or “Out” of phase) and antisymmetric (“AS”, solid thick line) modes.

where k_{PS} and k_{CPS} are the integer positive values assumed in Eqs. (13a) and (14a), respectively. For example, for $\upsilon = 0.5$, Eq. (14) defines the location at $L/3$, for which the frequencies of both primary mode (2 wavelengths $k_{PS} = 2$) and complementary mode ($k_{CPS} = 1$) are coincident with the third symmetric mode (wavelength L/3). The geometry of the three modal configurations is modified (the rank of Eq. (10) is reduced to 1), and a complex behavior similar to the symmetric case with $\xi_1 = 1/2$ can be observed. The difference between points of class “**a**” and “**b**” is that, while in the first case all points are representative of the same behavior occurring at each “antisymmetric” modal frequency α ($\xi_1 = 1/2$), in the second case there is only one frequency (and the family of its multiples) that, for a given location of the bar, satisfies equality (15).

From Fig. 5 it can be seen how the position of the vertical connector significantly affects the system behavior. In particular, while frequencies of symmetric and antisymmetric modes are unmodified, those of *PS* and *CPS* modes can change dramatically if the former is moved from the centerline toward the edges. For values of ξ_1 close to 0.5 the frequency of *PS* and *CPS* are almost coincident and close to the antisymmetric value, from which this modal bifurcation is originated. Half of the cable is practically at rest. On the contrary, as ξ_1 approaches the lateral restraints, the frequency of the *CPS* is “projected” towards higher values and the possibility of switching from *PS* to *CPS* when a slight variation of a driving force is exerted disappears. This fact also suggests that the response of a non-perfectly symmetric system can be significantly modified by the external geometry, along with the presence of perhaps unexpected modal characteristics. Moreover, regions of multiple solutions seem to suggest a rapid rise of complexity in the analyses.

3.3. Symmetric-cable system with $L_2 \neq L_1$ and rigid connection at mid-span

Two taut strings with different length but symmetrically located with respect to their center-line are coupled together by means of a secondary cable located at mid span. In particular, it was assumed: $H_1 = H_2 = H$, $\mu_1 = \mu_2 = \mu$, $L_2 \leqslant L_1$, $h = 1$, $l_* = L_1/2$, $l_2 = L_2/2$, and $\omega_{02} = (1 + \varepsilon)\omega_{01}$ with $\varepsilon \geqslant 0$.

The reduced frequencies of the upper reference cable $\alpha_{j,1}$, are equal to the infinite series of natural numbers $(1, 2, \ldots, j, \ldots, N)$; those of the secondary one can be referred to the first set by the ratio $\omega_{j,2}/\omega_{j,1} = (1+\varepsilon)$. The secondary notation (Fig. 1) was used in this example, in order to simplify the final equation system and avoid the dependence of l_1, l_2, etc. The modified expressions for $Y_{1,\ldots,4}$ and $A_{1,\ldots,4}$ are described through the expressions

$$Y_{1,2}(x_{1,2}) = A_{1,2}\sin\left(\frac{\alpha\pi}{L}x_{1,2}\right), \quad Y_{3,4}(x_{3,4}) = A_{3,4}\sin\left(\frac{\alpha f\pi}{L_2}x_{3,4}\right), \tag{16a, b}$$

where $L_1 = L$ for simplicity (note the coordinate normalization in Eq. (16b). Quantities (16a) and (16b) are still a solution to the general problem (3), provided that the frequency of the system ω is such that

$$\omega = \alpha\frac{\pi}{L}\left(\frac{H}{\mu}\right)^{0.5} = \alpha\omega_{01}, \quad f = L_2/L = 1/(1+\varepsilon). \tag{17a, b}$$

The quantity f (17b) represents the ratio between cable lengths and is a function of ε. By substituting Eqs. (16) and (17) into Eq. (3) and recalling the boundary conditions (2), the system matrix $\mathbf{S}$ can be written in the form

$$\mathbf{S} = \begin{Bmatrix} \sin\beta & -\sin\beta & 0 & 0 \\ 0 & 0 & \sin(f\beta) & -\sin(f\beta) \\ \sin\beta & 0 & -\sin(f\beta) & 0 \\ \cos\beta & \cos\beta & \cos(f\beta) & \cos(f\beta) \end{Bmatrix} \quad \text{with } \beta = \frac{\alpha\pi}{2}. \tag{18}$$

Similarly, the characteristic polynomial, associated with $\det[\mathbf{S}] = 0$, can be reduced to

$$p(\alpha) = \left\{\sin\left[\frac{\alpha\pi(1+f)}{2}\right]\right\}\left\{2\left[\cos\left(\frac{\alpha\pi(1+f)}{2}\right) - \cos\left(\frac{\alpha\pi(1-f)}{2}\right)\right]\right\}. \tag{19}$$

Eq. (19) has two main sets of roots, each one of which is related to the quantities in brackets. The first one ("S-A"), related to the sine expression—left part of Eq. (19), is connected to the set of in-phase symmetric modes. In this case the eigenvalue–eigenvector solution is modified by the presence of the shorter cable: the possibility of a perfectly "tuned" solution for $\varepsilon > 0$ (as in Figs. 3(a) and (b) is impossible and the reduced frequencies increase according to the relationship

$$\alpha_S = 2k\frac{1}{1+f} = 2k\frac{1+\varepsilon}{1-\varepsilon} \quad \text{with } k = 1, 2, \ldots, N, \tag{20a}$$

$$\mathbf{A}_S = \begin{cases} 0.5[1 \;\; 1 \;\; 1 \;\; 1]^{\mathrm{T}} & \text{for } k \text{ odd (in phase)}, \\ 0.5[1 \;\; 1 \;\; -1 \;\; -1]^{\mathrm{T}} & \text{for } k \text{ even (out of phase)}. \end{cases} \tag{20b}$$

These values of α ensure the symmetry of modes and the requirement of equilibrium at P_1 and P_2 (a force is transferred through the rigid connector). At these points a discontinuity in the derivative is necessary between the consecutive segments of the same cable, which must have opposite sign on the two sides.

The perfect equality (in modulus) of modal amplitudes can be similarly proved, which is responsible for the in-phase and out-of-phase eigenvector components (20b).

The second set of roots ("S-B"), related to the cosine expression, can be divided in two subsets. The first one (*I*) is the solution that corresponds to the antisymmetric mode of the upper cable, with frequency and amplitudes expressed by the expressions

$$\alpha_{AS,I} = 2k \quad \text{with } k = 1, 2, \ldots, N, \qquad \mathbf{A}_{AS,I} = 0.71[1 \;\; -1 \;\; 0 \;\; 0]^{\mathrm{T}}. \tag{21a, b}$$

For the equilibrium and the continuity at nodes $P1$ and $P2$ (18), the shorter cable must be at rest.

The second family of modes (*II*) is given by

$$\alpha_{AS,II} = \frac{2k}{f} = 2k(1+\varepsilon) \quad \text{with } k = 1, 2, \ldots, N, \qquad \mathbf{A}_{AS,II} = 0.71[0 \;\; 0 \;\; 1 \;\; -1]^{\mathrm{T}}. \tag{22a, b}$$

In both cases (21) and (22) the rank of $\mathbf{S}$ is 3 and no force is transmitted through the restrainer. A further reduction of rank for antisymmetric modes is not possible, unless ε is such that $\sin[k\pi(1+\varepsilon)] = 0$ (continuity at mid-span for Eq. (20a)), for a given k. This possibility can occur at higher modes, when the ratio between the two cables, f, is equal to the wavelength of a particular mode (note the similarity with Eq. (15)) and the convergence of three modal frequencies is attained (rank[$\mathbf{S}$] = 1).

All the modal frequencies are summarized in Fig. 6, as a function of the cable length ratio, f. Some characteristic eigenfunctions are also included. The modes are divided in symmetric (20) and antisymmetric (21,22) modes. For the former, in-phase and out-of-phase patterns of opposite cables are indicated. Nodes labelled as "**b**" are associated with the coexistence of more than one modal form (as an example, two of the possible solutions for $f = 0.5$ and $\alpha = 1/3$ are indicated). Nodes denoted by "**a**" are related to the antisymmetric/symmetric multiple modal form (multiplicity 3) for $f = 1$ (twin-cable systems); as f differs from the unitary value, the bifurcation among the three sets is evident (20–22). The relative increment of α, particularly for antisymmetric modes (22) and higher symmetric solutions, is strongly influenced by the reduction of length in the lower cable; as an example, for f in the range of 0.5–0.7, this class of modes tends to rapidly evolve to higher order.

4. Flexible connectors

The symmetric examples analyzed in Sections 3.1 and 3.2 were extended to the case of a non-rigid secondary restrainer. The new configuration is shown in Fig. 7. A linear spring of stiffness K was inserted between the center-lines of the two cables, allowing for a relative displacement between points $P1$ and $P2$ on the two cables, $\delta_{P_1P_2}$, simulating perhaps more realistically the behavior of a cross-tie. In Fig. 7, an additional extension to ground of the connector is also considered, with $K_G \neq K$ to allow for a generalized characterization of the problem (see Section 5).

The boundary conditions (2d) and (2e) need to be modified to take into account the presence of the spring elements. Details on the derivation of these equations and the system matrix are included in Appendix A.

The term $d_K = H/KL$ is a dimensionless positive parameter, relating the stiffness of the cable system (through H and L) to that of the P_1–P_2 connector. As $d_K \to 0$ the solution approaches the behavior discussed in Section 3 (rigid tie); the condition $d_K \to \infty$ is representative of two

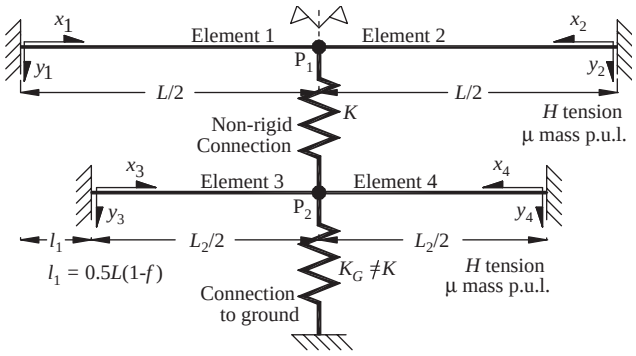

Fig. 7. Symmetric-cable system ($L_2 \leqslant L_1$) with non-rigid secondary connection simulated by a linear spring with stiffness K, extended to ground (with $K_G \neq K$).

disconnected taut-strings ($K \to 0$). Typical values of d_K were computed, considering examples of existing cross-tied cable networks; the interval of investigation can be generally defined between $d_K = 10^{-2}$ (long stays) and $d_K = 10^{0}$. Similarly, the ground parameter $d_G = H/K_G L$ relates the stiffness of the cable system to the second spring.

4.1. Solution to the twin-cable system without connection to ground

Under the conditions $d_G \to \infty$ and $f = 1$ ($L_2 = L_1$), the matrix $\mathbf{S}$ of Eq. (A5) can be simplified; the characteristic polynomial associated with $\det[\mathbf{S}] = 0$ becomes

$$p(\alpha) = \{\sin(\alpha\pi)\}\{[\cos(\alpha\pi) - 1] - \alpha\pi\, d_K \sin(\alpha\pi)\} \tag{23a}$$

or

$$p(\alpha) = \left\{\frac{\cos(2\alpha\pi) - 1}{2}\right\}\left\{\tan\left(\frac{\alpha\pi}{2}\right) + \alpha\pi\, d_K\right\}. \tag{23b}$$

Expression (24a) is immediately recognizable as Eq. (9) of the rigid system, as $d_K \to 0$. Also in this case two sets of roots can be identified: $p(\alpha) = \{p_{\text{“S-B”}}\}\{p_{\text{“S-A”}}\}$. The first one, denoted by “S-B”, is the solution to the left part of Eqs. (24), which represents the set of modes that, in the twin-cable system, is not influenced by the presence of the vertical connection (i.e., $\alpha = k$ with $k = 1, 2, \ldots, N$ and no internal force between P_1 and P_2). These are the modes of the isolated cable, as discussed in Section 3.1, symmetric (odd values of k—Fig. 2) and antisymmetric (even-valued, in which the in-phase and out-of-phase solutions can coexist—Fig. 3(a)).

The final expression for the set “S-A”, which represents the out-of-phase symmetric class of modes, modified by the imperfect rigidity, is linked to the solution of the transcendental expression

$$T(\alpha, d_k) = \tan\left(\frac{\alpha\pi}{2}\right) + \alpha\pi\, d_K = 0. \tag{24}$$

The general pattern is quite similar to the fundamental equation of cable vibration for elements with sag: an approximate solution to the equation $\tan(\gamma/2) - \gamma/2 = 0$ was found by Rohrs; details

can be found in Ref. [12]. A numerical algorithm was developed for the iterative solution of Eq. (24) as a function of the parameter d_K.

Fig. 8(a) depicts Eq. (24) for $d_K = 5.0, 0.5, 0.05, 0$, over the interval $1<\alpha<5$. The roots of $T(\alpha, d_k)$ can be divided in two classes: class "**a**" points, related to the condition $d_K = 0$ (rigid connector with $\alpha = 2, 4$); class "**b**" points, for which the solution depends on the spring stiffness. It is evident from this figure that the frequency values associated with "**b**" points are lower than those for $d_K = 0$. A general relative "down-shift" of these solutions towards lower α can be detected as the modal interval increases (compare $\mathbf{b_{1-3}}$ for $1<\alpha<3$, and $\mathbf{b_{3-5}}$ for $3<\alpha<5$). This tendency becomes much more pronounced in higher modes, in which all roots, for $d_K \neq 0$, tend to odd-valued frequencies, corresponding to symmetric components of "S-B".

The evolution of the reduced frequencies as a function of d_K and related to the 2nd, 4th, 6th and 8th symmetric modes, is presented in Fig. 9(a). Significant modifications of α with respect to a "disconnected system" can be observed for $d_K<0.3$ only. In fact, for higher values of d_K, the

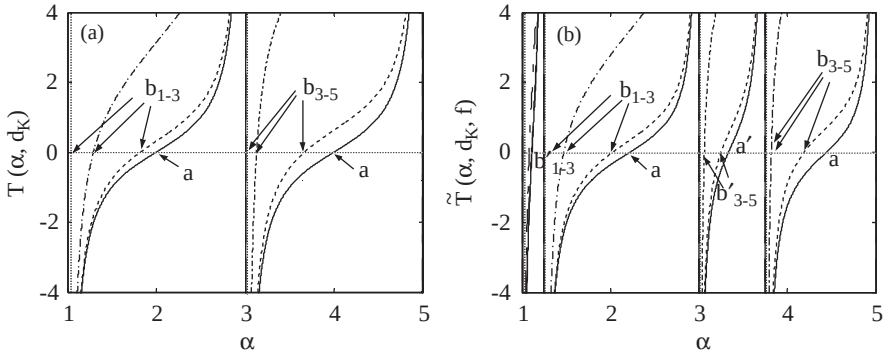

Fig. 8. Non-rigid symmetric-cable systems. Analysis of the transcendental equations (32,33) for different values of the stiffness parameter $d_K = H/KL$ in the interval $1<\alpha<5$: (a) $T(\alpha; d_k)$ for twin cables with $f = 1$; (b) $\tilde{T}(\alpha; d_k, f)$ for symmetric cables and $f = L_2/L_1 = 0.80$. $d_k = 5.0$ (- - -), $d_k = 0.5$ (– · –), $d_k = 0.05$ (– –), $d_k = 0$ (—).

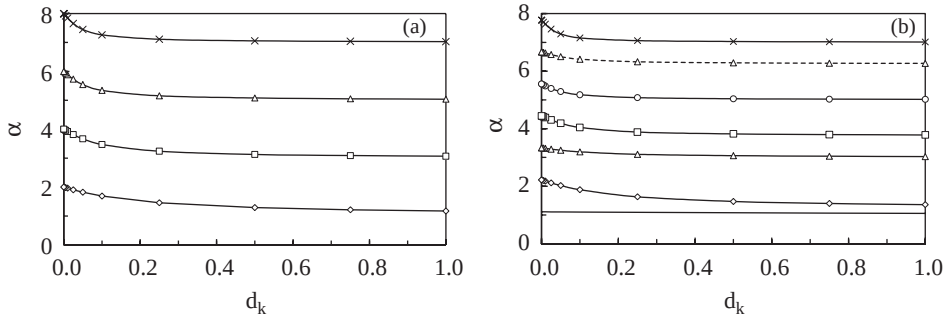

Fig. 9. Evolution of the normalized frequency, $\alpha = \omega/\omega_{01}$, as a function of the stiffness parameter $d_K = H/KL$ for non-rigid symmetric-cable systems: (a) 2nd (-◇-), 4th (-□-), 6th (-△-) and 8th (-×-) symmetric modes for twin cables with $L_2 = L_1$; (b) 1st (—), 2nd (-◇-), 3rd (-△-), 4th (-□-), 5th (-○-), 6th (···△···) and 7th (-×-) symmetric modes for symmetric cables and $f = L_2/L_1 = 0.80$.

solutions are almost coincident with the asymptotic behavior for $d_K \to \infty$, with the two cables vibrating independently. The down-shift property, highlighted in Fig. 11(a), can also be seen.

In Fig. 10 the modal components, $Y_r(x_r)$, for a high, an intermediate and a low value of d_K have been computed for the 2nd (2S) and the 4th (4S) symmetric modes. The 1st and 3rd symmetric are unaffected (Fig. 2). The variation of separation among the four segments at mid-span (Fig. 10) is a measure, in normalized form, of the relative displacement (A1) between the two cables,

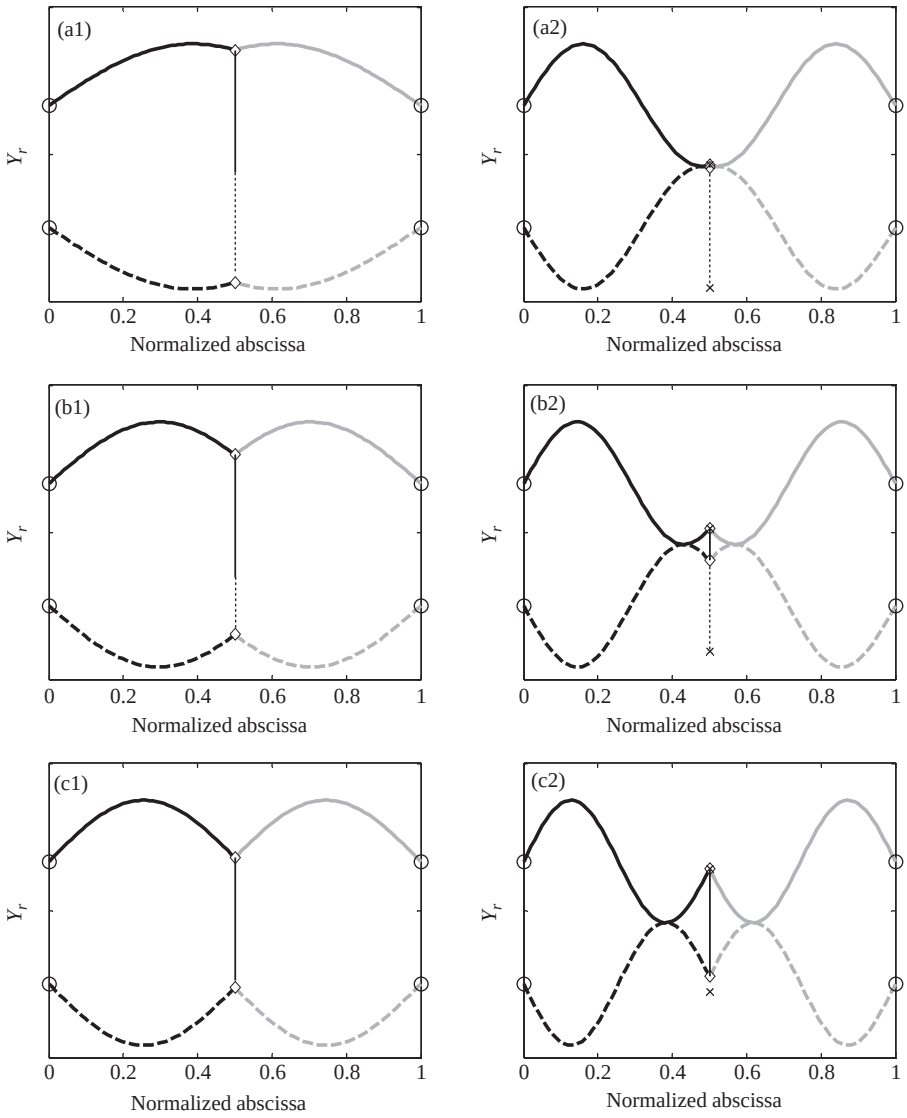

Fig. 10. Non-rigid twin-cable system ($f = 1$). Evolution of the Y_r eigenfunctions associated with the 2nd and 4th symmetric modes, 2S and 4S, as a function of the stiffness parameter d_k: (a1) mode 2S, $d_K = 0.50$, $\alpha = 1.29$; (a2) mode 4S, $d_K = 0.50$, $\alpha = 3.13$; (b1) mode 2S, $d_K = 0.10$, $\alpha = 1.69$; (b2) mode 4S, $d_K = 0.10$, $\alpha = 3.47$; (c1) mode 2S, $d_K = 0.01$, $\alpha = 1.96$; (c2) mode 4S, $d_K = 0.01$, $\alpha = 3.92$. Solid lines: Y_1, Y_2; dashed lines: Y_3, Y_4.

i.e., the elongation or contraction of the spring element. As the stiffness of the spring increases, with respect to cable characteristics, the relative distance between points $P1$ and $P2$ decreases. In particular for $d_K = 0.5$, the efficiency of the connection is so poor that the modal shape (and frequency) is essentially the same as the odd-numbered symmetric modes (i.e., for example, mode 2S is almost coincident with 1S). For higher modes, forces induced on the restrainer are more relevant and the relative displacements become larger (previously interpreted in terms of reduced frequencies and the "down-shift" effect of "**b**" points in Fig. 8(a)).

4.2. Solution to the symmetric cable system ($L_1 \neq L_2$) without connection to ground

Under the conditions $d_G \to \infty$ but $f \neq 1$, the polynomial associated with system (A5) becomes

$$p(\alpha) = \left\{\cos\left[\frac{\alpha\pi(1+f)}{2}\right] - \cos\left[\frac{\alpha\pi(1-f)}{2}\right]\right\} \cdot \left\{\sin\left[\frac{\alpha\pi(1+f)}{2}\right] + \alpha\pi\, d_K \cos\left[\frac{\alpha\pi(1+f)}{2}\right] + \alpha\pi\, d_K \cos\left[\frac{\alpha\pi(1-f)}{2}\right]\right\}, \tag{25}$$

where two sets of roots are identified: $p(\alpha) = \{p_{\text{"S-B"}}\}\{p_{\text{"S-A"}}\}$. The solution to $p_{\text{"S-B"}} = 0$ relates to the complete set of antisymmetric modes, independent of the normalized stiffness, also coincident with the case of the two isolated cables, in which no force is exerted by the vertical connector (see also Eq. (19)). The interesting set, identified as "S-A", can be equivalently rewritten as

$$p_{\text{"S-A"}}(\alpha) = \left\{\cos\left[\frac{\alpha\pi(1+f)}{2}\right] - \cos\left[\frac{\alpha\pi(1-f)}{2}\right]\right\}\left\{0.5\tan\left(\frac{\alpha\pi f}{2}\right) + 0.5\tan\left(\frac{\alpha\pi}{2}\right) + \alpha\pi\, d_K\right\} \tag{26}$$

with $p_{\text{"S-A"}}(\alpha) = \{p_{\text{"S-A1"}}\}\{p_{\text{"S-A2"}}\}$. It can be shown that the solutions to $p_{\text{"S-A1"}} = 0$ are the same as those to $p_{\text{"S-B"}} = 0$; on the contrary $p_{\text{"S-A2"}}$ is related to the class of modes equivalent to Eqs. (21) and (22) for $d_K = 0$. In this case, the transcendental expression, $\tilde{T}(\alpha, d_k, f)$, similar to Eq. (24) for $f = 1$, becomes

$$\tilde{T}(\alpha, d_k, f) = 0.5\tan\left(\frac{\alpha\pi f}{2}\right) + 0.5\tan\left(\frac{\alpha\pi}{2}\right) + \alpha\pi\, d_K = 0. \tag{27}$$

Fig. 8(b) depicts the general behavior of these roots, for different values of $d_K \neq 0$ in the interval $1 < \alpha < 5$ and a system with $f = L_2/L = 0.8$ ($\varepsilon = 0.25$).

In the figure class "**a**" and "**a′**" points are coincident with the rigid-connector case. There are two solutions between the vertical asymptotes corresponding to odd values of $\alpha = 1, 3, 5$, associated with modes denoted by a solid thin line in Fig. 6. New asymptotes can be observed among these intervals, linked to the vanishing of Eq. (27). However, it can be also observed from the analysis of Fig. 6 that, as f decreases, this tendency disappears beyond the cross-over points of multiple solutions.

Therefore, there will be two possible solutions also for $d_K \neq 0$ (class "**b**" and "**b′**" points). A new property is also evident, in addition to the already mentioned frequency down-shift for higher modes ($\mathbf{b_{1-3}}$ for $1 < \alpha < 3$, and $\mathbf{b_{3-5}}$ for $3 < \alpha < 5$). The relative position of the new asymptotes, corresponding to the solution of antisymmetric modes in which only the shorter cable is excited (Eq. (22)), tends to get closer to the upper frequency limit as the mode number increases. As a

result, a relative increment in the frequency can be detected, as for example between $\mathbf{b}'_{\mathbf{1-3}}$ for $1<\alpha<3$ and $\mathbf{b}'_{\mathbf{3-5}}$ for $3<\alpha<5$.

Fig. 9(b) presents, as an example, the evolution of the reduced frequency α, numerically determined through Eq. (27) as a function of d_K for a symmetric system with $f = 0.80$, equivalent to Fig. 9(a). All symmetric modes (1st to 7th) are affected by d_K, due to the loss of perfect similarity between the taut-cables (through f), in contrast to the previous case. It also reveals that the frequency increment of the system with respect to the single cable solution is higher (only for even-numbered symmetric modes–out of phase), due to the general trend of "**b**" and "**b′**" points.

In Fig. 11 the modal components, $Y_r(x_r)$, for $f = 0.8$ ($\varepsilon = 0.25$) and a high, an intermediate and a low value of d_K, have been computed for the 1st (1S, in-phase) and the 2nd (2S, out-of-phase) symmetric modes, determined by the roots of the polynomial depicted in Fig. 8(b). By comparison of these modes with the equivalent behavior for twin cables ($f = 1$), described in Fig. 10, the lack of symmetry among modal amplitudes is more evident for high values of the normalized stiffness (a "soft" system).

5. Solution to symmetric-cable system ($L_2 \neq L_1$) with connection to ground

In this generalized case the full matrix (A5) must be considered ($L_2 \neq L_1, d_K$ and d_G finite). The characteristic polynomial can be divided in two parts, $p(\alpha) = \{p_{\text{"S-B"}}\}\{p_{\text{"S-A"}}\}$, i.e.,

$$p_{\text{"S-B"}}(\alpha) = \{\cos[\alpha\pi\,(1+f)] - \cos[\alpha\pi(1-f)]\}, \tag{28a}$$

$$p_{\text{"S-A"}}(\alpha) = 0.25\left\{\left[\tan\left(\frac{\alpha f\pi}{2}\right) + \tan\left(\frac{\alpha\pi}{2}\right) + 2\alpha\pi\, d_K\right] + \left[\frac{d_K}{d_G}\tan\left(\frac{\alpha\pi}{2}\right) + \frac{1}{2\alpha\pi\, d_G}\tan\left(\frac{\alpha\pi}{2}\right)\tan\left(\frac{\alpha f\pi}{2}\right)\right]\right\}. \tag{28b}$$

As before, the solution to $p_{\text{"S-B"}} = 0$ is related to the complete set of antisymmetric modes, independent both of d_K and d_G in which no force is exerted by both vertical connectors and coincident with the case of the two isolated cables.

The interesting set, labeled "S-A" and associated with the symmetric modes, is related to the solution of a transcendental equation, similar to that previously defined in the case with no restrainer to ground (Eq. (26)), with an additional factor due to the extension of the cross-tie to ground. A mapping of solutions to $p_{\text{"S-A"}} = 0$ was computed, by simultaneously varying f, d_K and the ground parameter d_G. Fig. 12 summarizes the solutions to Eq. (28b) for $f = 0.80$ (constant), with variables $0.01<d_K<1$ and d_G (between $d_G = 10d_K$ and $d_G = 0.01d_K$) in the interval $1<\alpha<5$.

The first analyzed case corresponds to the condition $d_G = d_K$ (equal stiffness, Fig. 12(b)). Vertical asymptotes represent the solution associated with the symmetric modes of the two individual cables $\alpha = 1, 3$ and $\alpha = 1/f, 3/f$. For a central connector sufficiently rigid ($d_K = 0.01$), the presence of ground restrainer increases the frequency (upward shifting) for $3<\alpha<3/f$ and $3/f<\alpha<5$ (higher modes), as indicated by nodes **a** and **a′**. Depending on d_K (and, consequently, d_G) more than one solution can exist among the asymptotes (e.g., **a**-type points for $1/f<\alpha<3$ in

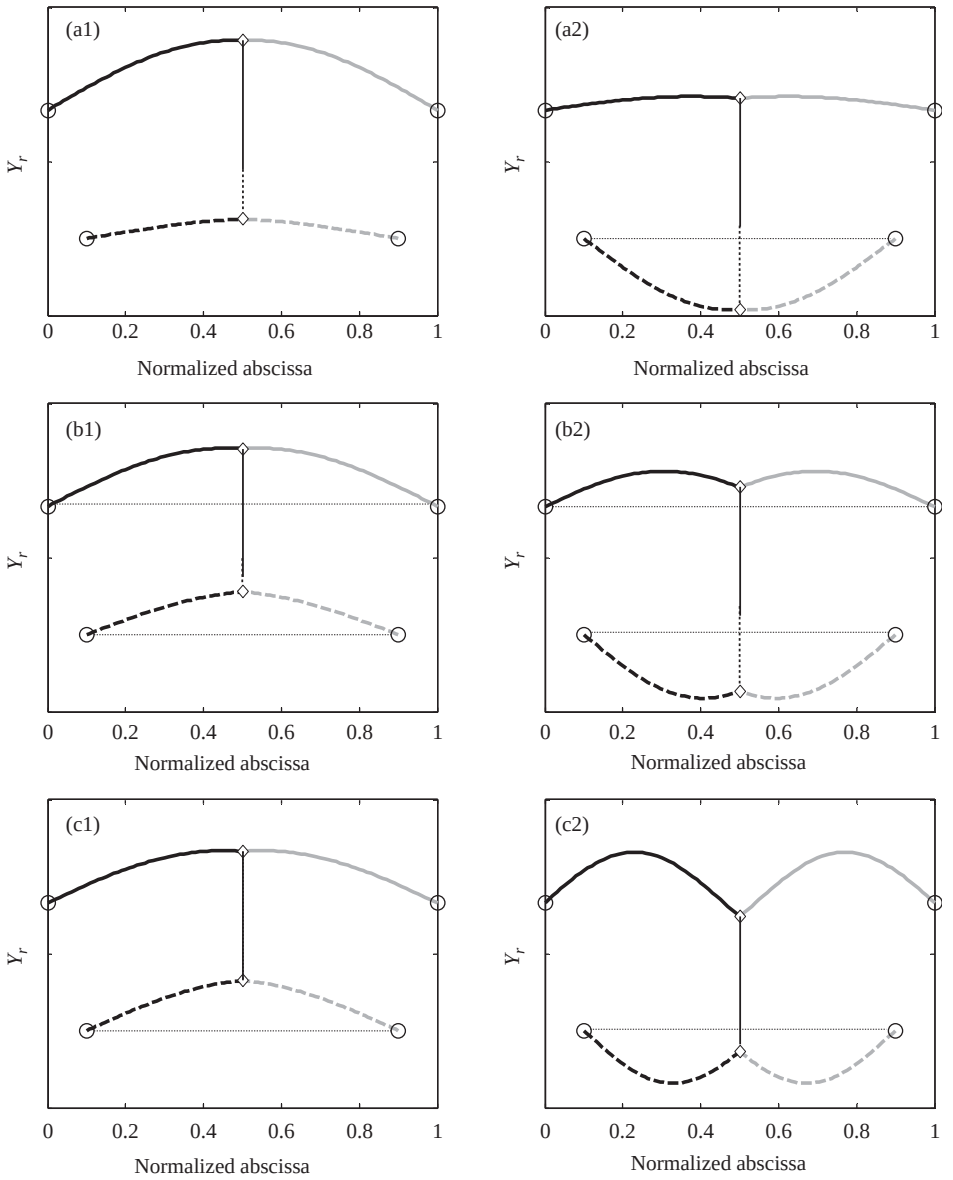

Fig. 11. Non-rigid symmetric-cable system ($f = 0.80$). Evolution of the Y_r eigenfunctions associated with the 1st and 2nd symmetric modes, 1S and 2S, as a function of the stiffness parameter d_k: (a1) mode 1S, $d_K = 1.50$, $\alpha = 1.05$; (a2) mode 2S, $d_K = 1.50$, $\alpha = 1.32$; (b1) mode 1S, $d_K = 0.25$, $\alpha = 1.09$; (b2) mode 2S, $d_K = 0.25$, $\alpha = 1.63$; (c1) mode 1S, $d_K = 0.01$, $\alpha = 1.11$; (c2) mode 2S, $d_K = 0.01$, $\alpha = 2.18$. Solid lines: Y_1, Y_2; dashed lines: Y_3, Y_4.

Fig. 12(b)). Nevertheless, this behavior tends to disappear at higher α or higher d_K (flexible connection and points **b**).

For $d_G = 0.1 d_K$ (Fig. 12(c)) the stiffness of the ground connector is considerably higher than that of the internal tie; both **a** and **b** solutions are present among asymptotes. In particular, points

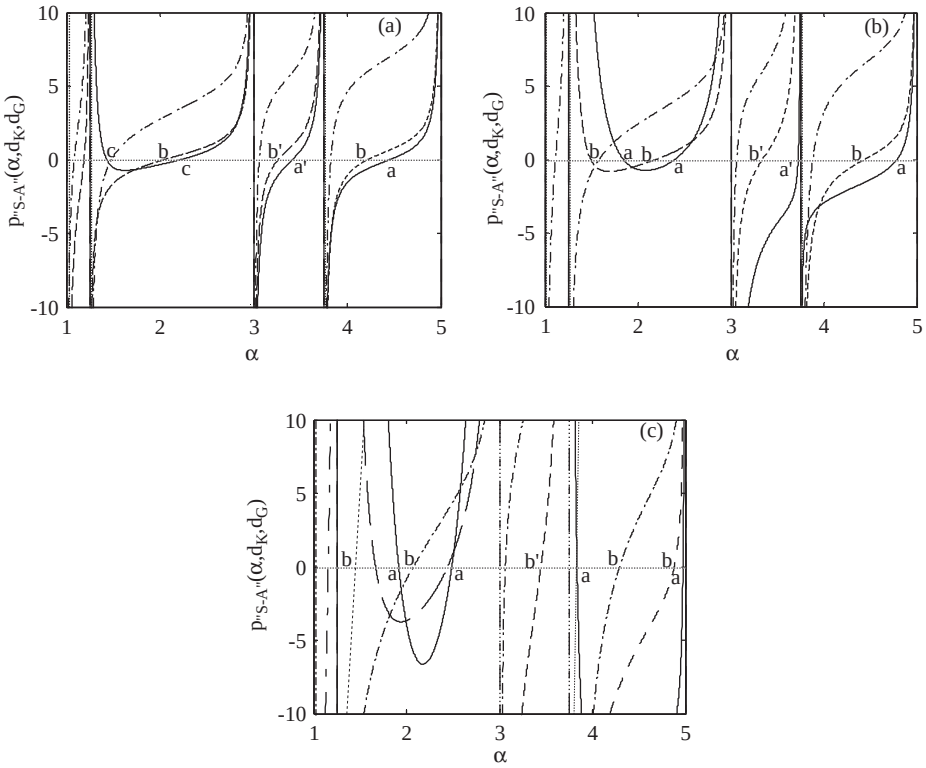

Fig. 12. Non-rigid symmetric-cable systems ($f = 0.80$) with connector to ground. Analysis of Eq. (33b), p"$_{S\text{-}A}$" (α, d_K), in the interval $1<\alpha<5$ as a function of d_K, for (a) $d_G = 10\,d_K$, (b) $d_G = d_K$, (c) $d_G = 0.1\,d_K$; $d_k = 5.0$ (- - -), $d_k = 0.5$ (– · –), $d_k = 0.05$ (– –), $d_k = 0$ (—).

a correspond to a case in which the connection to ground (P_2) can be considered as an almost fixed point (compared to the flexibility of the internal system, through d_K). The upper solution (**a**) in the interval $1/f<\alpha<3$ tends to $\alpha = 2/f = 2.5$, with the upper cable at rest and symmetric eigenfunctions associated with the lower cable with wavelength equal to $L_2/2$ (qualitatively similar to Fig. 3(b)). On the contrary the lower solution **a** in the same interval tends to a similar mode with $\alpha = 2$ in which the situation is reversed.

In case $d_G = 10d_K$ (Fig. 12(a)) the link to ground is relatively more flexible. At higher modes the solution is almost coincident with the case in which no ground connection is present (Fig. 8(b)) as in points **a**, **a**′ and **b**, **b**′. In addition, for $1/f<\alpha<3$ and high values of d_K the two cables are almost disconnected from each other, i.e., isolated. For low d_K, since the internal restrainer is still "active", a hybrid solution is detected (points **c**): the limit behavior is characterized by a mode in which the modal amplitude of each element is similar (in phase—smaller **c** solution; out of phase—larger **c** solution).

Fig. 13 presents the modal eigenfunctions associated with the 1st (1S, in-phase) and 2nd (2S, out-of-phase) symmetric modes, for a non-rigid symmetric-cable system, elastically restrained to ground, with cable length ratio $f = 0.8$ and a constant value of $d_K = 0.25$, by varying the ground parameter

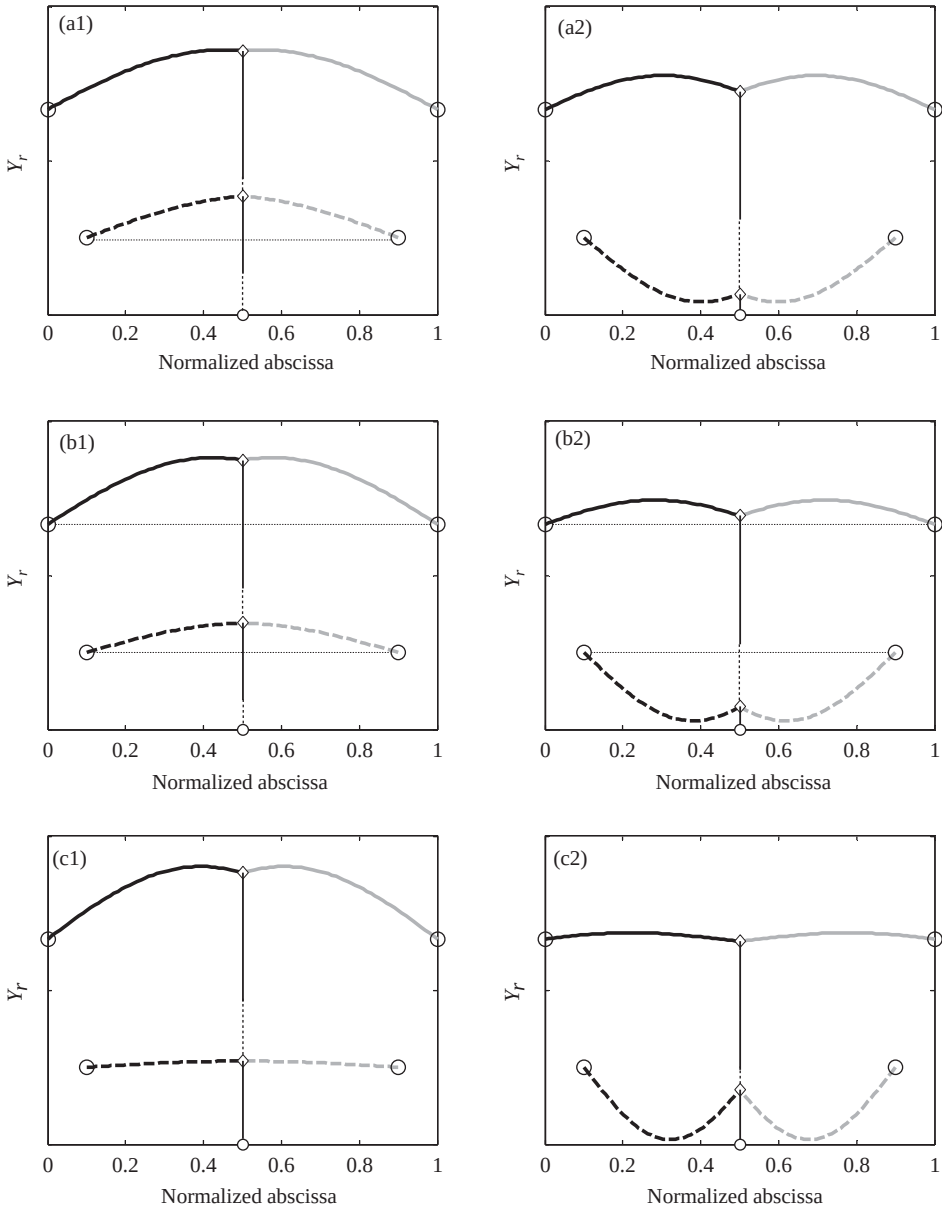

Fig. 13. Non-rigid symmetric-cable system ($f = 0.80$ and $d_K = 0.25$) with connection to ground. Evolution of the Y_r eigenfunctions associated with the 1st and 2nd symmetric modes (1S, 2S), as a function of the ground parameter d_G: (a1) mode 1S, $d_G = 10d_K = 2.50$, $\alpha = 1.11$; (a2) mode 2S, $d_G = 10\,d_K = 1.50$, $\alpha = 1.65$; (b1) mode 1S, $d_G = d_K = 0.25$, $\alpha = 1.18$; (b2) mode 2S, $d_G = d_K = 0.25$, $\alpha = 1.77$; (c1) mode 1S, $d_G = 0.1\,d_K = 0.03$, $\alpha = 1.27$; (c2) mode 2S, $d_G = 0.1\,d_K = 0.03$, $\alpha = 2.25$. Solid lines: Y_1, Y_2; dashed lines: Y_3, Y_4.

d_G as a function of d_K. It is worth observing that when the stiffness of the spring to ground is relatively high ($d_G = 0.1d_K$), the localized response of one single cable at a time is emphasized: the amplitude is increased or largely reduced on either cable, according to the frequency.

Parametric studies on the combined influence of the stiffness parameters d_K, d_G and f (cable length ratio) on the reduced modal frequencies, $\alpha = \omega/\omega_{01}$, were conducted for selected modes. An increment in the frequency is generally observed, by simultaneously adapting the values of d_K and d_G. For the sake of brevity the results are not reported here.

6. Conclusions

An analytical procedure for the assessment of cable network behavior has been implemented in this paper using taut cable theory. This procedure solves the free-vibration problem of a system of stays, interconnected by a set of cross-ties. The introduction of transverse elements, usually adopted as countermeasure to suppress oscillations induced by external actions, has been investigated, by solving the dynamic equations for a set of simplified examples. From these results it is evident that even a geometrically simple system can rapidly become complex in terms of number and type of solutions. A numerical procedure has been developed for the general assessment of the modal characteristics. These analyses have contributed to the generation of a study background that has been used in a companion paper [13] for investigations concerning real systems, including the generalization of the present method and the numerical procedure to large problems. This approach has been applied to cable network systems of an actual bridge, along with comparison among different configurations of cross-tied networks, providing observations about the mitigation of large-amplitude stay vibrations of specific examples towards design applications.

The proposed method is preferred to a finite-element-based numerical analysis of a cable system, since some of the physical characteristics can be predicted and deduced from the general theory (interpretation of the results for large systems and comparison with the basic mechanics associated with simplified examples [13]).

The effectiveness of the proposed method, shown by the examples and in Ref. [13], is another significant aspect, capable of detecting the presence of multiple eigenvectors in symmetric networks.

Sensitivity studies, in which the number, the configuration and the location of connectors need to be almost routinely modified, can be improved through the proposed procedure, since the effort that is necessary to redefine a network system is much lower than that associated with a finite element simulation in which a redistribution of the nodes and the elements is required. While not considered here, the effect of the mass of the cross-tie systems can be readily considered by the addition of point masses at the connector locations.

The limitations of this approach are connected to the fact that effects of cable geometry (sag) are neglected as well as local characteristics of the network (e.g., the connection between cable and restrainer). In addition, the performance of the cross-ties is assumed as symmetric, simulated by means of simplified linear spring connectors.

Appendix A. Derivation of matrix

In Section 4, the internal compatibility equation (2d) between $P1$ and $P2$ is defined in accordance with the convention and notation as in Fig. 7, by relating the internal force to the

elongation (or contraction) of the spring with stiffness K, i.e. $F_S/K = \delta_{P_1P_2}$, or

$$\frac{H_1\left(\left.\frac{\partial y_1}{\partial x_1}\right|_{x_1=l^*} + \left.\frac{\partial y_2}{\partial x_2}\right|_{x_2=L_1-l^*}\right)}{K} = y_3(x_3 = l^*) - y_1(x_1 = l^*). \tag{A.1}$$

The force F_S is derived from the equilibrium at $P1$ on the upper cable, after considering Eqs. (16) for the $Y_{1,2}$ and $Y_{3,4}$ expressions and the following simplifications: $\omega_{02} = (1+\varepsilon)\omega_{01}$, $L_2 \leqslant L_1$, $H_2 = H_1 = H$, $l^* = L_1/2 = L/2$. Eq. (A.1) can be rewritten as

$$\frac{H}{L}\alpha\pi\left[A_1\cos\left(\frac{\alpha\pi}{2}\right) + A_2\cos\left(\frac{\alpha\pi}{2}\right)\right] = K\left[A_3\sin\left(\frac{\alpha f\pi}{2}\right) - A_1\sin\left(\frac{\alpha\pi}{2}\right)\right]. \tag{A.2}$$

In the presence of the additional restrainer between $P2$ and the ground, the force equilibrium condition (2e) is also modified, by defining as $F_G = -K_G y_{21}(l^*)$ the additional restoring force due to this element (Fig. 7):

$$H_1\left(\left.\frac{\partial y_1}{\partial x_1}\right|_{x_1=l^*} + \left.\frac{\partial y_2}{\partial x_2}\right|_{x_2=L_1-l^*}\right) + H_2\left(\left.\frac{\partial y_3}{\partial x_3}\right|_{x_3=l_2} + \left.\frac{\partial y_4}{\partial x_4}\right|_{x_4=L_2-l_2}\right) = K_G(-y_{21}(l^*)). \tag{A.3}$$

The force F_G is derived from the equilibrium of the two-cable system. Similarly, expression (A.3) can be rewritten as

$$\frac{H}{L}\alpha\pi\left[(A_1+A_2)\cos\left(\frac{\alpha\pi}{2}\right) + (A_3+A_4)\cos\left(\frac{\alpha f\pi}{2}\right)\right] = -K_G A_3\sin\left(\frac{\alpha f\pi}{2}\right). \tag{A.4}$$

Matrix (6c) becomes

$$\mathbf{S} = \begin{Bmatrix} \sin\beta & -\sin\beta & 0 & 0 \\ 0 & 0 & \sin(f\beta) & -\sin(f\beta) \\ 2\beta\, d_K\cos\beta + \sin\beta & 2\beta\, d_K\cos\beta & -\sin(f\beta) & 0 \\ \cos\beta & \cos\beta & \cos(f\beta) + \dfrac{\sin(f\beta)}{2\beta\, d_G} & \cos(f\beta) \end{Bmatrix}, \tag{A.5}$$

where $\beta = \alpha\pi/2$, $d_K = H/KL$ (normalized stiffness), $d_G = H/K_G L$ (ground parameter) and f is defined as in Eq. (17b).

References

[1] M. Matsumoto, N. Shiraishi, H. Shirato, Rain-wind induced vibration of cable-stayed bridges, *Journal of Wind Engineering and Industrial Aerodynamics* 43 (1999) 2011–2022.

[2] J.A. Main, N.P. Jones, H. Yamaguchi, Characterization of rain-wind-induced stay-cable vibrations from full-scale measurements, *Proceedings of the Fourth International Symposium on Cable Dynamics*, Montreal, Canada, 2001, pp. 235–242.

[3] N.J. Gimsing, *Cable Supported Bridges; Concept and Design*, Wiley, New York, 1983.

[4] J.A. Main, N.P. Jones, Free vibrations of a taut cable with attached damper. I: linear viscous damper, *American Society of Civil Engineers, Journal of Engineering Mechanics* 128 (2002) 1062–1071.

[5] F. Ehsan, R.H. Scanlan, Damping stay cables with ties, *Proceedings of the Fifth US–Japan Bridge Workshop*, 1990, pp. 203–217.

[6] G. Hirsch, Cable vibration overview, *Proceedings of the Eighth International Conference on Wind Engineering* (ICWE8), The University of Western Ontario, London, Canada, 1991, pp. 453–464.
[7] M. Virlogeux, Cable vibrations in cable-stayed bridges, in: A. Larsen (Eds.), *Bridges Aerodynamics*, A.A. Balkema, Rotterdam, 1998, pp. 213–233.
[8] H. Yamaguchi, L. Jayawardena, Analytical estimation of structural damping in cable structures, *Journal of Wind Engineering and Industrial Aerodynamics* 41–44 (1992) 1961–1972.
[9] H. Yamaguchi, H.D. Nagahawatta, Damping effects of cable cross ties in cable-stayed bridges, *Journal of Wind Engineering and Industrial Aerodynamics* 54/55 (1995) 35–43.
[10] A. Zingoni, An efficient computation scheme for the vibration analysis of high tension cable nets, *Journal of Sound and Vibration* 189 (1999) 55–79.
[11] S. Mesarovich, D.A. Gasparini, Dynamic behavior of nonlinear cable system (I and II), *Journal of Engineering Mechanics, American Society of Civil Engineers* 118 (5) (1990) 890–903 and 904–920.
[12] H.M. Irvine, *Cable Structures*, MIT Press, Cambridge, 1981.
[13] L. Caracoglia, N.P. Jones, In-plane dynamic behavior of cable networks. Part 2: prototype prediction and validation, *Journal of Sound and Vibration* 279 (3–5) (2005) 993–1014.